European Review for Medical and Pharmacological Sciences 2023; 27: 2571-2579

Image findings of tendon sheaths affected by diffuse tenosynovial giant cell tumors of the skull base

S.-S. ZHAO, J.-L. CHENG, E.-Y. GAO, J. BAI, Y. ZHANG

The First Affiliated Hospital of Zhengzhou University, Zhengzhou City, Henan Province, China

Abstract. – OBJECTIVE: This study investigated radiographic images and the differential diagnosis of intracranial diffuse tenosynovial giant cell tumor (D-TGCT) in order to better understand the disease and improve the rate of preoperative diagnosis.

PATIENTS AND METHODS: Images and clinical data of patients with D-TGCT were retrospectively analyzed. Routine Computer Tomography (CT), routine Magnetic Resonance Imaging (MRI), and contrast-enhanced MRI were performed for nine cases. Susceptibility-weighted imaging (SWI) was also performed for one case.

RESULTS: We reviewed nine patients (6 males and 3 females) aged between 24 and 64 years, with a mean age of 47.33 ± 14.92 years. The most frequent complaints were hearing loss (5/9, 55.6%), pain (4/9, 44%), masticatory symptoms (2/9, 22.2%), and mass (4/9, 44.4%), with a mean duration of 22 ± 21.43 months. All cases were centered on the base of the skull, and showed hyper-density soft-tissue mass with osteolytic bone destruction on CT. The tumor signal mainly showed iso-intensity or hypo-intensity on T1WI compared with that in the brain parenchyma in all patients. On T2WI, nine lesions mainly showed hypo-intensity. Among these nine lesions, three displayed cystic region showing hyper-intensity on T2WI and hypo-intensity on T1WI (Figure 2A, 2B) in the lesion. Nine lesions showed hypo-intensity on DWI sequences. SWI images presented low signal in two cases, showing the "flowering effect". Nine patients showed heterogeneous enhancement, and two patients had meningeal thickening.

CONCLUSIONS: Intracranial D-TGCT is extremely rare, but must be differentiated from other tumors. Osteolytic bone destruction in the area of the skull base with hyper-density soft-tissue mass and hypo-intensity on T2WI images are indicative of D-TGCT.

Key Words:
Tenosynovial giant-cell tumor, Intracranial, Tomography, X-ray computed, Magnetic resonance imaging.

Introduction

Diffuse tenosynovial giant-cell tumor (D-TGCT), also called Pigmented villonodular synovitis, is a benign proliferative disease of the synovium that usually involves joints and tendon sheaths[1]. D-TGCT occurs in large joints of the extremities, of which a single joint is most involved[2]. The tumor can be destructive. D-TGCT was initially reported to be an inflammatory disease related to chromosomal translocations detected by cytogenetics[3]. Research also suggests that chronic inflammation may cause the disease[4], and that repeated trauma and hemarthrosis are possible risk factors[5].

The current best treatment option is surgical resection. The cell biology of D-TGCTs indicates that they have a malignant tendency[6], and they are prone to malignant transformation after multiple recurrences[7]. The lesions can grow longitudinally around the tendon to form tiny satellite lesions. If the clinician does not have a comprehensive understanding of the tumor and the surgical resection fails to consider this feature, the small satellite lesions around the tumor may not be removed and can lead to tumor recurrence[8]. Thus, preoperative MRI diagnosis and differential diagnosis are particularly important. If the imaging diagnosis is D-TGCT, attention should be paid to surrounding satellite lesions and the resection extended to minimize the chance of tumor recurrence as much as possible to prevent lesions from becoming malignant.

D-TGCT rarely occurs in the temporomandibular joint (TMJ); most case reports in literature describe disease of the skull base. In our study, several cases were collected and reviewed in our hospital. Here we describe their radiologic imaging, clinical appearance, and treatment in order to raise awareness of the disease.

Corresponding Author: Jingliang Cheng, MD; e-mail: fccchengjl@zzu.edu.cn

Patients and Methods

Subjects

We selected nine patients whose D-TGCT diagnoses were confirmed by surgery and pathology in our hospital from July 2015 to December 2021. Clinical features including age, sex, symptoms, radiological imaging, and pathological findings were recorded (Table I).

Imaging Examination Methods

Routine CT, conventional, and contrast enhancement MRI were performed in nine cases, and the case 2 was examined with SWI. CT scans were performed using GE Discovery 64-slice spiral CT machine with a slice gap of 5 mm and a slice thickness of 5 mm. MR images of patients, scanned on 3.0-T MRI scanners (Magnetom Trio TIM/Prisma, Siemens Healthcare, Germany), were retrieved from the Picture Archive and Communication System at the hospital. The sequence acquisition parameters were as follows:

- 2D sequence T1-weighted [repetition time (TR): 250 ms; echo time (TE): 2.5 ms] in the sagittal plane and cross-sectional scanning;
- the turbo spin echo (SE) sequence T2-weighted imaging (TR 4500 ms, TE 100 ms) in the cross-sectional plane, a layer thickness 5 mm, no spacing interval, and two excitation imaging.

On axial diffusion-weighted imaging (DWI), a SE echo planar imaging sequence was used with TR 3,700 ms and TE 102 ms, b-values of 0 and 1,000, a layer thickness of 5 mm, and a layer spacing of 1.8 mm. During enhanced scanning, patients were injected with contrast agent [gadopentetate dimeglumine (Beijing Beilu Pharmaceutical Co., China)] at a dose of 0.2 ml/kg.

Image Analysis

All images were jointly read by two senior diagnostic radiologists who observed the lesion location, size, shape, adjacent bone changes, signal characteristics, and reinforcement mode of TGCT, recorded the results separately, discussed and compared them, and then reached a consensus.

Surgery and Pathological Examination

Seven patients underwent surgical total resection. Two patients underwent CT-guided biopsy at first go to hospital and chose surgical total resection when the size of tumor changed. All lesions underwent routine paraffin-embedded sectioning and HE staining.

Statistical Analysis

SPSS 22.0 statistical analysis software (IBM Corp., Armonk, NY, USA) was used for data processing. Statistical results were expressed as mean ± standard deviation. The incidence of hearing loss and the differences in CT and intraoperative performance between the two groups were compared using Chi-squared test. A value of $p<0.05$ was the criterion for statistical significance.

Results

Patient Characteristics

Patient clinical information is presented in Table I. We reviewed nine patients (six males and three females) between 24 and 64 years old, of mean age 47.33 ± 14.92 years. Five cases occurred on the right side and four cases occurred on the left. The most frequent complaints were hearing loss (5/9, 55.6%), pain (4/9, 44%), masticatory symptoms (2/9, 22.2%), and a mass (4/9, 44.4%), with a mean symptom duration of 22 ± 21.43 months.

Radiological Characteristics

The shape, size, and maximum diameter plane of the enhanced tumor on MRI imaging

The tumor manifested as irregular shape masses, grew diffusely, and infiltrated the surrounding tissues. The size of the tumor was 32-60 mm, and the maximum diameter was the upper-to-lower diameter, which was significantly larger than the transverse diameter and anterior-to-posterior diameter (Table II).

Density of computed tomography

All cases present soft tissue masses of mixed density with higher density area and osteolytic bone destruction expansion into the skull base bone (Figure 1G, 1H) and unclear boundary. The CT findings are summarized in Table II.

Signal of magnetic resonance imaging

The tumor presented mainly iso-intensity or hypo-intensity on T1WI compared with the signal of the brain parenchyma in all patients (Figure 1A, 2B). On T2WI, nine lesions mainly showed

Table I. General information of nine cases of D-TGCT at the base of the skull.

No.	Age	Sex	Nationality	Side	Chief complaint	Duration of symptom month	Operation resection	Prognosis
1	56	M	Han	right	Hearing loss, pre-auricular mass	8	Total resection	Loss to follow-up
2	60	M	Han	left	Facial nerve paralysis, Hearing loss, Pre-auricular mass	48	Total resection	Recurrence-free survival (1 year)
3	64	F	Han	right	Confused when chewing	1	Total resection	Recurrence-free survival (1 year)
4	59	M	Han	left	Temporal mass	60	Total resection	Recurrence-free survival (1 year)
5	24	M	Han	right	Earache, Hearing loss	3	Biospy, Total resection	Recurrence-free survival (2 year)
6	46	F	Han	left	Earache, Hearing loss	36	Total resection	Recurrence-free survival (3 year)
7	36	F	Han	left	Temporal mass	12	Total resection	Recurrence-free (3 year) survival
8	54	M	Han	right	Mastoid process pain when chewing	24	Biospy, Total resection	Recurrence-free survival (3 year)
9	27	M	Han	left	Earache, Hearing loss	6	Total resection	Loss to follow-up

hypo-intensity (Figure 1B). Among these nine lesions, three displayed cystic regions showing hyper-intensity on T2WI and hypo-intensity on T1WI (Figure 2A, 2B) in the lesion. Nine lesions showed hypo-intensity on DWI sequences (Figures 1C, 2D). SWI images presented low signal in case 2, showing the "flowering effect" (Figure 1F). Nine patients showed heterogeneous enhancement (Figure 1D). The MRI findings are summarized in Table II.

Surrounding invasion of tumors

Temporal meningeal enhancement around the tumor was observed in two patients (Figure 1E). In four patients, the lesions grew into the external auditory meatus after destroying the anterior wall (Table II). In one case, the tumor involved the facial nerve root with enhancement, forming soft tissue masses in the cerebellar-pontine region (case 1). The tumor invaded the bone of the mastoid region in two cases (Table II). Compression of the Eustachian tube was observed in nine patients with mastoiditis. According to the extent of bone destruction on CT images, the patients were divided into Group A (involving external auditory meatus, mastoid process, and tympanum) and Group B (not involving external auditory meatus, mastoid process, and tympanum). The incidence of hearing loss in Group A (5/6) was higher than that in Group B (0/3; $p < 0.05$, $\chi^2=5.625$). There was no significant difference between group A (5/1) and Group B (3/3; $p > 0.05$, $\chi^2=0.563$) between CT images and intraoperative diagnosis of bone destruction.

Tumor Recurrence and Follow-Up

The tumor had no recurrence at three years after the operation in three cases. Three patients had no recurrence two years after the operation. In one case, the tumor had no recurrence one year after the operation. The remaining two patients were lost to follow-up after the operation (Table I).

Pathological Radiological Manifestations

Postoperative pathological examination revealed foam cells, multinucleated giant cells, and hemosiderin-laden macrophages. The pathological diagnosis was a diffuse giant cell tumor of the tendon sheath (Figure 1I).

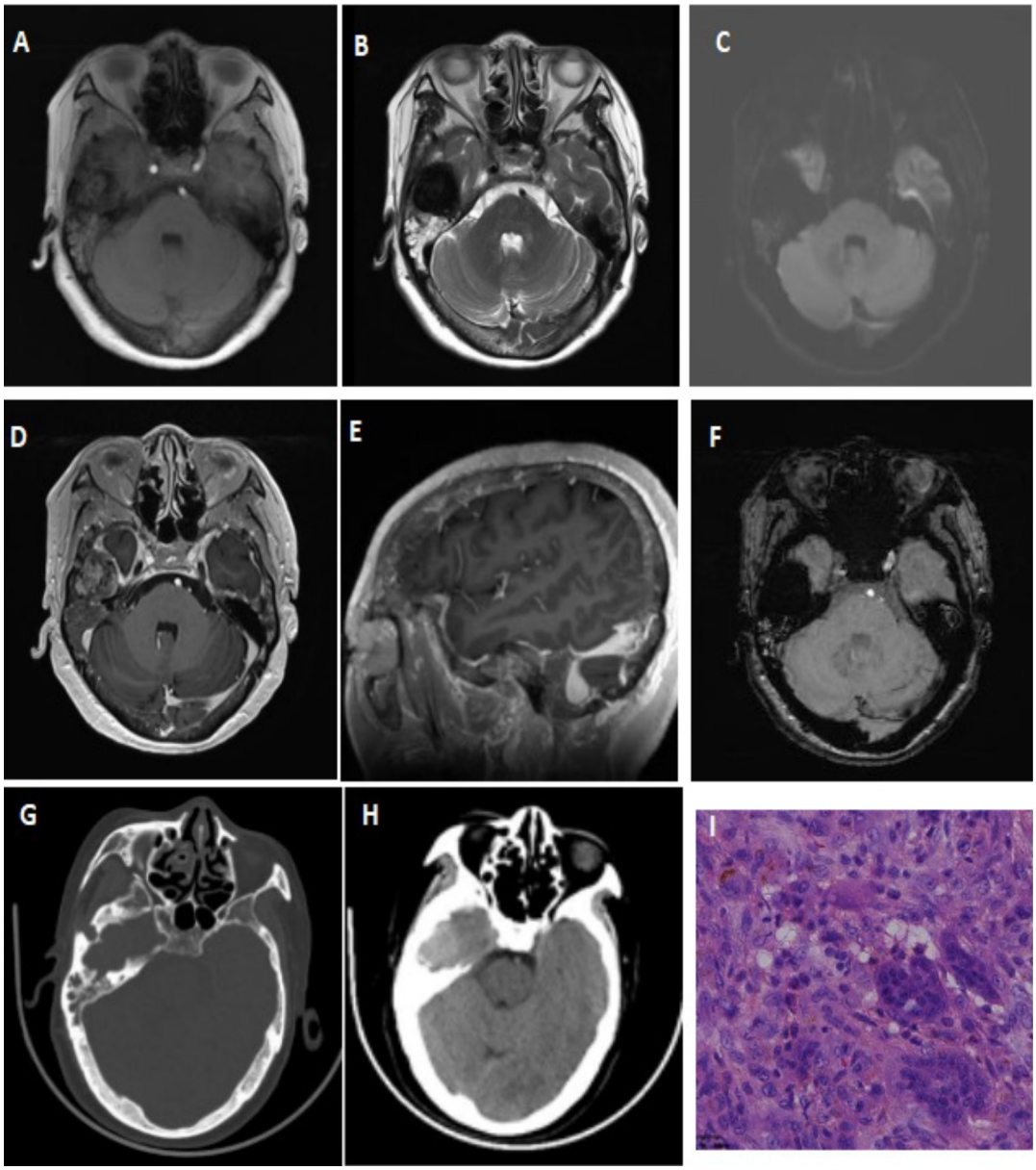

Figure 1. A 64-year-old female with diffuse tenosynovial giant cell tumor (D-TSGCT) in right temporomandibular joint (TMJ). **A**, T1; (**B**), T2; (**C**), DWI (b=100); (**D-E**), Gd-DTPA; (**F**), SWI; (**G**), HRCT (bone window); (**H**), HRCT (soft tissue window); (**I**), Postoperative pathological examination (400×).

Discussion

The 2013 WHO classification of D-TGCT soft-tissue tumors[9] includes the following groups: segmental (single nodule), diffuse (multiple nodules), and malignant, among which the segmental type is the most common[10,11]. D-TGCT can occur at any age but is more common in adults aged 30-50 years[12]; one patient in our case series was diagnosed to have it at the age of 24, consistent with a previous study[13]. D-TGCT often involves the fingers and knee joints, followed by the ankles, hips, elbows, shoulder joints, and spine[2]. D-TGCT of the TMJ is very rare, and involvement of the skull base is even rarer. In this study, in all nine cases, the tumor occurred in the temporal skull base and was diffuse.

Symptoms in patients with this disorder are nonspecific and include a painful or painless pre-auricular mass, TMJ symptoms, and hearing impairment[14]. Local numbness may occur in some cases, due to compression of the trigeminal nu-

cleus and facial nerve. Age of onset, progressive hearing impairment, and TMJ symptoms were specific in this case.

Pathologically, most D-TGCT were rich in monocytes, foam cells, multinucleated giant cell, and hemosiderin-laden tissue macrophages[15], consistent with the results of this study. In addition, other studies[10] have shown that there is a 1p13 chromosomal translocation in most D-TGCT cases, with overexpression of the colony-stimulating factor 1 (*CSF1*) gene. Colony-stimulating factor receptor 1 (CSF1R) is a protein located on the cell surface that controls the generation and differentiation of macrophages. Overexpression of CSF1, a ligand for CSF1R, can form a CSF1 gradient that recruits CSF1R-expressing cells (such as macrophages) involved in tumor formation, thereby promoting tumor growth through a "paracrine landscape" effect[16] in D-TGCT. This mechanism provides a potential site for targeted drug action by CSF inhibitors to treat D-TGCT.

Accurate preoperative diagnostic imaging can facilitate more precise treatment plan formulation and prognostic evaluation. D-TGCT usually showed an irregular mass with unclear boundaries, which was related to its aggressive biological behavior. MRI images showed diverse appearances as a result of different proportions of hemosiderin, fibers, lipids, stroma, and cellular components[17]. MRI provides better characterization and

Table II. Imaging findings of 9 Patients of P9 cases of D-TGCT at the base of the skull.

			CT			MR			
Case	Size (mm)	Shape	Osteolytic bone destruction	Hyper-density soft tissue	Density	T1	T2	DWI	Enhancement
1	37*50*32	Mass	TB, MT	(+)	Heterogeneous	Iso-intensity, Hypo-intensity	Hypo-intensity (main)	Hypo-intensity	Moderately heterogeneous
2	58*45*36	Mass	TB, MD, EAC	(+)	Heterogeneous	Iso-intensity, Hypo-intensity	Hypo-intensity (main)	Hypo-intensity	Moderately heterogeneous
3	33*35*27	Mass	TB	(+)	Heterogeneous	Iso-intensity, Hypo-intensity	Hypo-intensity (main)	Hypo-intensity	Moderately heterogeneous
4	61*54*47	Mass	TB, ZB	(+)	Heterogeneous	Iso-intensity, Hypo-intensity	Hypo-intensity (main)	Hypo-intensity	Moderately heterogeneous
5	46*47*39	Mass	TB, EAC	(+)	Heterogeneous	Iso-intensity, Hypo-intensity	Hypo-intensity (main)	Hypo-intensity	Moderately heterogeneous
6	32*36*39	Mass	TB, SB, EAC	(+)	heterogeneous	Iso-intensity, Hypo-intensity	Hypo-intensity (with cystic signal)	Hypo-intensity	Moderately heterogeneous
7	57*60*49	Mass	TB, ZB	(+)	Heterogeneous	Iso-intensity, hypo-intensity	Hypo-intensity (main)	Hypo-intensity	Moderately heterogeneous
8	42*39*52	Mass	TB, SB, MD, TP	(+)	Heterogeneous	Iso-intensity, Hypo-intensity	Hypo-intensity (with cystic signal)	Hypo-intensity	Moderately heterogeneous
9	42*39*39	Mass	TB, EAC, MT	(+)	Heterogeneous	Iso-intensity, Hypo-intense	Hypo-intensity (with cystic signal)	Hypo-intensity	Moderately heterogeneous

*TB temporal bone, SB sphenoid bone, ZB zygomatic bone, EAC external auditory canal, MT mastoid, MD mandible, TP tympanum. (+) hyper-density soft-tissue mass. The size of the lesion was measured on enhanced MRI examination.

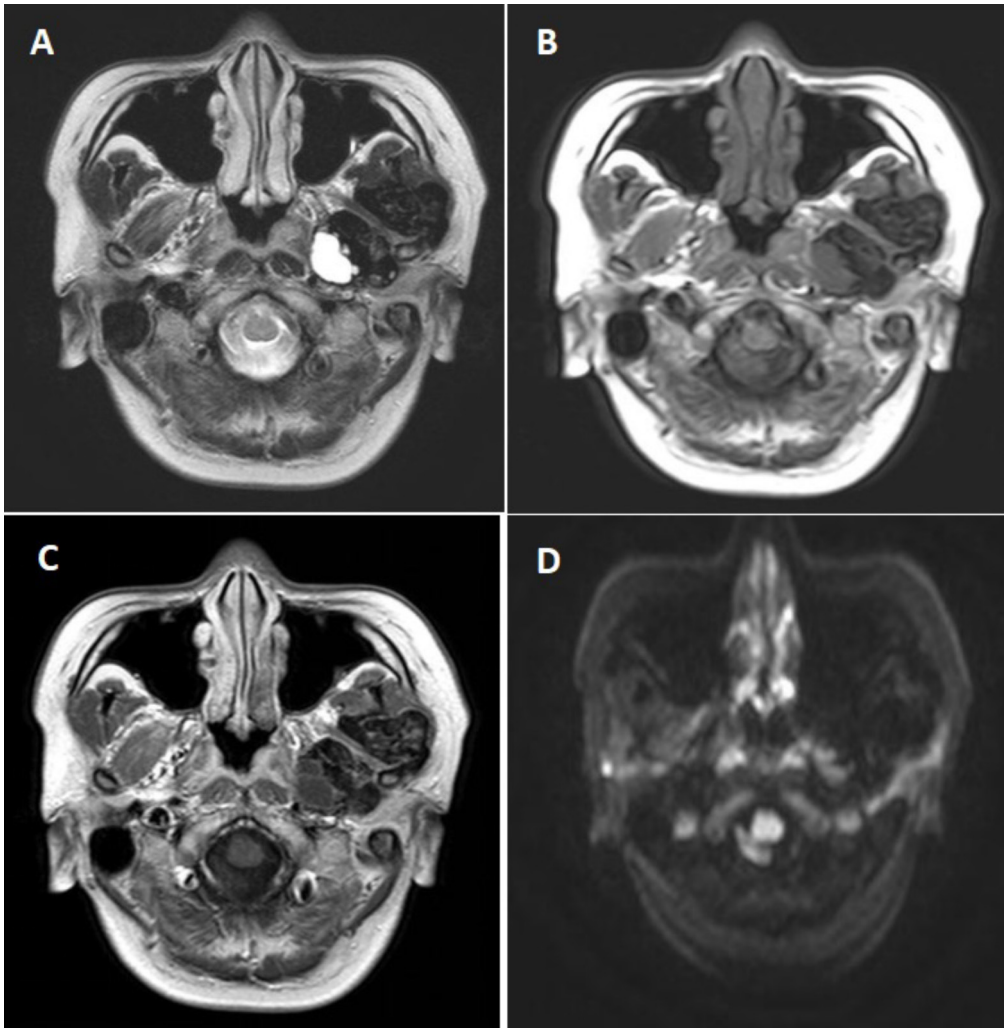

Figure 2. Magnetic resonance imaging (MRI) of a 46-year-old man with diffuse tenosynovial giant cell tumor (D-TS-GCT) in left TMJ. **A**, T2; (**B**), T1; (**C**), Gd-DTPA; (**D**), DWI (b=100).

delineation of the tumor, showing intermediate and hypo-intensity signal intensity on T1-weighted imaging, and multiple intensity (hypo-intensity, hyper-intensity, iso-intensity) on T2-weighted sequencing[18]. The low signal area on T2WI represents hemosiderin with paramagnetic effect, which can shorten T2 relaxation time[19]. Iso-intensity and hyper-intense areas represent tumor tissue and cystic lesion on T2WI[20], respectively. In this study, nine patients have been found to have the hypo-intensity area, two patients the cystic hyper-intensity area and seven patients the iso-intensity area on T2WI. Extended hypo-intensity (the "flowering effect") on DWI or SWI sequences were caused by the presence of hemosiderin with paramagnetic effect. On CT imaging, classic features of D-TGCT usually presented as soft tissue masses of mixed density with higher density area as a result of hemosiderosis[22] and destructive expansion into the skull base bone, consistent with the imaging results in our study. Neale et al[23] suggested that the destruction of bone in D-TGCT lesions was mainly associated with the activation of osteoclast differentiation by monocyte and multinucleated giant cell-expressed antigenic phenotypes, similar to those of osteoclasts. All cases showed bone destruction of the skull base, two of which invaded the skull base through the destruction area of the tumor in this study. The extent of lesions and bone destruction can be observed on CT examinations[22]. In this study, there was no significant difference between CT images and intraoperative diagnosis of bone destruction. The incidence of hearing loss in patients with in-

volvement of periotic bone was higher than that in patients without periotic bone involvement, suggesting that the extent of bone on CT scan is consistent with the symptoms. GCTBs of the cranial and facial bones most commonly affects the temporal and sphenoid bones[24]. GCTBs of the lateral skull base are often locally aggressive and can invade nearby critical structures[25]. It is believed[26] that these tumors arise in these areas because the bones of the mandible, sphenoid, ethmoid, and parts of the temporal bone form largely through the process of endochondral ossification. In contrast, the other cranial bones (i.e., frontal and parietal bones) arise from intramembranous ossification and are less frequently affected by GCTB. In this study, nine patients had no involvement of the frontal bone and parietal bone. De Schepper et al[27] believe that capillaries proliferate to large numbers in D-TGCT lesions, resulting in significant enhancement of the lesions on imaging. Nine patients demonstrated mild enhancement which, may be due to capillary hyperplasia and hemosiderin deposition which limited the extravasation of the contrast agent.

In clinical practice, it is difficult to distinguish the intra- from the extra-articulation type of lesion, due to the complicated anatomy of the TMJ[28]. TMJ D-TGCT has been divided into three types in terms of imaging features, including a bone-centric type, soft-tissue type, and intra-osseous type. The cases in our study are mainly of the bone-centric type, which usually occurs in the craniofacial bone around the TMJ, showing extensive bone destruction, an incomplete bone shell, and surrounding soft tissue mass[28]. Our cases and previous reports[28,29] suggest that lesions of the bone-centric type are larger than those of the other types, possibly due to the longer disease course. Preservation of the articular surface and unaffected TMJ function in the early stage of the disease may delay the patient's consultation. In this study, only two patients had TMJ symptoms.

The main differential diagnoses of TMJ D-TGCT include giant cell tumor (GCT) of bone, synovial chondromatosis, rheumatoid arthritis (RA), aneurysmal bone cyst (ABC), and cholesteatoma. Bone GCT often involves the long bones of the extremities, mainly showing expansive growth, and is soap bubble-like, without calcification or ossification. Synovial osteochondromatosis is common in the synovial membrane of large joints. Multiple calcified nodules in the tumor on CT can be used as a differential diagnosis. The above two diseases lack hemosiderin deposition. RA often involves multiple joints and mainly manifests as decalcification and joint gap narrowing. ABC is characterized by dilated osteolytic bone lesions accompanied by a thin sclerotic border on CT or MRI, and typical fluid-fluid levels, showing hyper-intensity in the upper layer and hypo-intensity in the bottom layer on T2WI. Cholesteatoma also applies to mixed solid cystic mass arising deep in the temporal bone, which can lead to erosion of the skull. In most of the cases[30], at least one small bone was severely damaged, thus breaking the continuity of the small bone chain. Accurate diagnosis before surgery can be challenging, because of the extremely low incidence of D-TGCT. In our study, CT showed a hyper-density soft-tissue mass, and MRI showed hypo-intensity or mixed low signal on T1WI and mixed low signal or low signal on T2WI and some tumors had cystic changes. These features may be unique to the D-TGCT of TMJ, combined with the medical history and histopathological features.

Post-treatment D-TGCT recurrence rates depend on the affected joint and the duration of follow-up[31,32]. The principal treatment strategies for D-TGCT are surgical resection of the diseased bone and extensive synovectomy[30]. However, in complete resection, it is difficult to conserve adjacent joint function, because of the invasive nature of the disease. Consequently, adjuvant external beam radiation therapy is required when complete resection is not possible with surgery. D-TGCT is thought to be a tumor of unspecified behavior, is histologically benign, and rarely metastasizes[33].

Conclusions

Intracranial D-TGCT is extremely rare but must be differentiated from other tumors. Osteolytic bone destruction in the area of the skull base with hyper-density soft-tissue mass and hypo-intensity on T2WI images are indicative of D-TGCT.

Conflict of Interest

The Authors declare that they have no conflict of interests.

Authors' Contributions

Shanshan Zhao drafted the manuscript. Shanshan Zhao, Jie Bai, and Yong Zhang analyzed and interpreted data. Shanshan Zhao and Eryuan Gao acquired the data. Shanshan Zhao and Jie Bai conceived and designed the study. All authors read and approved the final version of the manuscript.

Ethics Approval

The study was approved by the Ethics Committee of the First Affiliated Hospital of the Zhengzhou University of China. The privacy and safety of subjects were adequately protected in accordance with clinical study guidelines (Protocol code: 2019-KY-231).

Informed Consent

Informed consent was obtained from all individual participants in the study.

ORCID ID

Shanshan Zhao: 0000-0001-7290-9238.
Jingliang Cheng: 0000-0002-6996-329X

References

1) Carlson ML, Osetinsky LM, Alon EE, Inwards CY, Lane JI, Moore EJ. Tenosynovial giant cell tumors of the temporomandibular joint and lateral skull base: review of 11 cases. Laryngoscope 2017; 127: 2340-2346.
2) Sheppard DG, Kim EE, Yasko AW, Ayala A. Giant-cell tumor of the tendon sheath arising from the posterior cruciate ligament of the knee: a case report and review of the literature. Clin Imaging 1998; 22: 428-430.
3) West RB, Rubin BP, Miller MA, Subramanian S, Kaygusuz G, Montgomery K, Zhu S, Marinelli RJ, Luca AD, Kelly ED, Goldblum JR, L Corless CL, Brown PO, Gilks CB, Nielsen TO, Huntsman D, Rijn M. A landscape effect in tenosynovial giant-cell tumor from activation of CSF1 expression by a translocation in a minority of tumor cells. Proc Natl Acad Sci USA 2006; 103: 690-695.
4) Oehler S, Fassbender HG, Neureiter D, Meyer-Scholten C, Kirchner T, Aigner T. Cell populations involved in pigmented villonodular synovitis of the knee. J Rheumatol 2000; 27: 463-470.
5) Myers BW, Masi AT. Pigmented villonodular synovitis and tenosynovitis: A clinical epidemiologic study of 166 cases and literature review. Med 1980; 59: 223-238.
6) Anazawa U, Hanaoka H, Shiraishi T, Morioka H, Morii T, Toyama Y.Similarities between giant cell tumor of bone, giant cell tumor of the tendon sheath, and pigmented villonodular synovitis concerning ultrastructural cytochemical features of multinucleated giant cells and mononuclear stromal cells. Ultrastruct Pathol 2006; 30: 151-155.
7) Zhou J, Zhang HZ, Jang ZM, Tang L, Liu L, Chen J. Clinicopathological analysis of malignant tenosynovial giant cell tumor. Journal of Clin and Exp Pathol 2012; 28: 1119-1123.
8) Li C, Wei JN, Zhao JH, Tian GL, Zhu J, Pan YW, Li YC. Long-term follow-up results of 86 cases of giant cell tumor of the tendon sheath of the upper extremity. Chinese J of Hand Surg 2001; 17: 151-154.
9) Fletcher CD, Bridge JA, Hogendoorn PC, Mertens F. WHO Classification of Tumors of Soft Tissue and Bone. 4th ed. Lyon, France: International Agency for Research on Cancer (IARC) 2013: 97-103.
10) Li B, Wang C, Zhang MM. Imaging features of giant cell tumor of the tendon sheath. Chinese J Radiology 2015; 49: 454-457.
11) Shi Sk, Zhang P, Zhang L, Zhou L, Cai ZG. Comparative analysis of MRI signs and pathology of giant cell tumor of the tendon sheath. Intl J Med Radiology 2019; 42: 341-345.
12) Tap WD, Wainberg ZA, Antony SP, Ibrahim PN, Zhang C, Healey JH, Chmielowski B, Staddon AP, Cohn AL, Shapiro GI, Keedy VL, Singh AS, Puzanov I, Kwak EL, Wagner AJ, Von Hoff DD, Weiss GJ, Ramanathan RK, Zhang JZ, Habets G, Zhang Y, Burton EA, Visor G, Sanftner L, Severson P, Nguyen H, Kim MJ, Marimuthu A, Tsang G, Shellooe R, Gee C, West BL, Hirth P, Nolop K, Rijn MVD, Hsu HH, Peterfy C, Lin PS, Starksen ST, Bollag G. Structure-guided blockade of CSF1R kinase in tenosynovial giant-cell tumor. N Engl J Med 2015; 373: 428-437.
13) He Q, Zan X, Chen F, You C, Xu JG. Pigmented villonodular synovitis of the temporomandibular joint with skull base extension: a retrospective case series. Sci Rep 2022; 12: 5763.
14) Joshi K, Huang B, Scanga L, Buchman C, Chera BS. Postoperative radiotherapy for diffuse pigmented villonodular synovitis of the temporomandibular joint. Am J Otolaryngol 2015; 36: 106-113.
15) Ge YX, Guo G, You YQ, Li YZ, Xuan YH, Jin ZW, Yan G. Magnetic resonance imaging features of fibromas and giant cell tumors of the tendon sheath: differential diagnosis. Eur Radiol 2019; 29: 3441-3449.
16) West RB, Rubin BP, Miller MA, Subramanian S, Kaygusuz G, Montgomery K, Zhu S, Marinelli RJ, Luca AD, Kelly ED, Goldblum JR, Corless CL, Brown PO, Gilks CB, Nielsen TO, Huntsman D, Rijn MV. A landscape effect in tenosynovial giant-cell tumor from activation of CSF1 expression by a translocation in a minority of tumor cells. Proc Natl Acad Sci USA 2006; 103: 690-695.
17) Lynskey SJ, Pianta MJ. MRI and thallium features of pigmented villonodular synovitis and giant cell tumors of tendon sheaths: a retrospective single-center study of imaging and literature review. Br J Radiol 2015; 88: 1056.
18) Freeman JL, Oushy S, Schowinsky J, Sillau S, Youssef AS. Invasive giant cell tumor of the lateral skull base: a systematic review, meta-analysis, and case illustration. World Neurosurg 2016; 96: 47-57.
19) Zhang HF, Luo HS, Yang H, Peng JD, Gong HH. MRI diagnosis of diffuse type tenosynovial giant cell tumor. J Practical Radiol 2018; 34: 477-479.

20) Li B, Wang C, Zhang MM. Imaging features of giant cell tumor of the tendon sheath. Chinese J of Radiol 2015; 49: 454-457.

21) Wan JMC, Magarelli N, Peh WCG, Guglielmi G, Shek TWH. Imaging of giant cell tumor of the tendon sheath. Radiol Med 2010; 115: 141-151.

22) Bemporad JA, Chaloupka JC, Putman CM, Roth TC, Tarro J, Mitra S, Sinard JH, Sasaki CK.Pigmented villonodular synovitis of the temporomandibular joint: diagnostic imaging and endovascular therapeutic embolization of a rare head and neck tumor. AJNR Am J Neuroradiol 1999; 20: 159-162.

23) Neale SD, Kristelly R, Gundle R, Quinn JM, Athanasou NA. Giant cells in pigmented villonodular synovitis express an osteoclast phenotype. J Clin Pathol 1997; 50: 605-608.

24) Shen Y, Ma C, Wang L, Li J, Wu Y, Sun J. Surgical management of giant cell tumors in the temporomandibular joint region involving lateral skull base: a multidisciplinary approach. J Oral Maxillofac Surg 2016; 74: 2295-2311.

25) Freeman JL, Oushy S, Schowinsky J, Sillau S, Youssef AS. Invasive giant cell tumor of the lateral skull base: a systematic review, meta-analysis, and case illustration. World Neurosurg 2016; 96: 47-57.

26) Morriss-Kay GM. Derivation of the mammalian skull vault. J Anat 2001; 199: 143-151.

27) De Schepper AM, Hogendoorn PC, Bloem JL. Giant cell tumors of the tendon sheath may present radiologically as intrinsic osseous lesions. Eur Radiol 2007; 17: 499-502.

28) Wang JG, Liu J, He B, Gao L, Zhang L, Liu J. Diffuse Tenosynovial Giant Cell Tumor Around the Temporomandibular Joint: An Entity With Special Radiologic and Pathologic Features. J Oral Maxillofac Surg 2019; 77: 1022.e1-22.e39.

29) Son SM, Park YS, Choi CH, Lee HC, Lee OJ, Woo CG. Extra-articular tenosynovial giant cell tumor of diffuse type in the temporal area with brain parenchymal invasion: a case report. Br J Neurosurg 2018; 32: 688-690.

30) Salvinelli F, Trivelli M, Greco F, Linthicumjr FH. Cholesteatomatous otitis media: histopathological changes-A post-mortem study on temporal bones. Eur Rev Med Pharmacol Sci 1999; 3: 183-187.

31) Byers PD, Cotton RE, Deacon OW, Lowy M, Newman PH, Sissons HA, Thomson HA. The diagnosis and treatment of pigmented villonodular synovitis. J Bone Joint Surg Br 1968; 50: 290-305.

32) Schwartz HS, Unni KK, Pritchard DJ. Pigmented villonodular synovitis. A retrospective review of affected large joints. Clin Orthop Relat Res 1989; 247: 243-255.

33) Asano N, Yoshida A, Kobayashi E, Yamaguchi T, Kawai A. Multiple metastases from histologically benign intraarticular diffuse-type tenosynovial giant cell tumor: a case report. Hum Pathol 2014; 45: 2355-2358.